Determination of Size Distribution of Elliptical Microvessels from Size Distribution Measurement of Their Section Profiles[1]

R.A. KRASNOPEROV[2]*‡ AND A.N. GERASIMOV†

Scientific Research Center, †Department of Computer Science and Medical Statistics, I.M. Sechenov Moscow Medical Academy, Russia 119881; and ‡Proxima Technology, Ltd., Moscow, Russia 123154

In transmission electron microscopy, microvessels (MVs) are studied as profiles on ultrathin sections. To determine MV sizes from measurements made on MV profiles, an assumption must be made about MV shape, a circular cylinder being used to approximate the latter on limited lengths. However, this model is irrelevant in case MVs have some flatness. The elliptical cylinder model is preferable, although relationships between the cylinder profile (two-dimensional; 2D) and its true (three-dimensional; 3D) sizes are not yet known. We have obtained the 2D/3D functions that express the relationships between such profile sizes as the minor radius (Y), major radius (X), axial ratio (X/Y), area (S), and perimeter (P) on the one hand, and the corresponding MV sizes (Y_0, X_0, X_0/Y_0, S_0, and P_0) on the other. The 2D/3D functions make it possible to derive elliptical MV sizes from section profile size distributions, probability density functions (PDFs) for the latter being determined. We have applied the 2D/3D functions in studying axial ratios of thyroid hemocapillaries. A factual X/Y frequency histogram has been constructed and fitted by theoretical X/Y PDFs plotted for different sets of capillary sizes. The thyroid capillaries have been revealed to be clustered, 72.7% of them having $X_0/Y_0 \approx 1.6$, 17.6%, $X_0/Y_0 \approx 1.0$, and 9.7%, $X_0/Y_0 \approx 3.2$. The proposed technique is instrumental in precise modeling of microcirculatory network geometry. Exp Biol Med 228:84–92, 2003

Key words: stereology; elliptical cylinder; microvessel shape model; size distribution; thyroid gland

In the body organs, microvessels (MVs), blood and lymphatic vessels with radii of up to 100–150 μm, form microcirculatory systems that ensure a selective supply of necessary substances to the cells and remove catabolic wastes into circulation. In the endocrine glands, MVs are additionally involved in hormone transfer to systemic circulation. Physiologically, microcirculation is so important that MVs are certainly a vital area of research in experimental biology and medicine. Transmission electron microscopy (TEM) remains one of the main methods for studying MV ultrastructure. With TEM, the size parameters of MVs and of their components are measured on section profiles.

Stereological design-based methods do not require assumptions about object shapes, and they find an increasingly wide use in modern research (e.g., Ref. 1). Currently available design-based methods are meant, above all, for unbiased estimation of the number and volume of particles of arbitrary shape. As for estimating sizes of section profiles of elongated objects including MVs, existing design-based methods cannot be applied. Therefore, model-based methods continue to be used in studies of MV size distributions. Specifically, correction coefficients are introduced to minimize the bias caused by nonperpendicular sectioning of MVs (2–4). This makes it possible to determine MV sizes from measurements of their section profiles, the shape of a MV on limited lengths of its basal surface being approximated by a straight circular cylinder. Confident enough estimates of MV sizes can be achieved, their accuracy being comparable with that of MV shape approximation.

However, MVs cannot always be regarded as circular cylinders. They may have a significant ellipticity of perpendicular section profiles. Although we have found only one article whose findings experimentally prove this point of view (Ref. 5: venular MVs in the pig heart are studied by optical sectioning, i.e., by changing the focal plane through the thickness of the histological section; their mean axial ratio is equal to 1.32 [postcapillary venules] or 1.38 [venules of the next order]), general considerations suggest that microcirculatory networks might be capable of acquiring an ellipticity in the regions of comparably low blood or lymph hydraulic pressure, as well as in places of increased outer pressure brought to bear by the surrounding tissue. Consequently, the revealed ellipticity of the coronary venules can

[1] This paper was presented at the 2001 FASEB Meeting, Orlando, FL. (FASEB J 15:A119, 2001).

[2] To whom requests for reprints should be addressed at 20a-107, L. Tolstoy Street, Pushkino, Moscow Region, 141206 Russia. E-mail: rkrasnoperov@yandex.ru

Received December 17, 2001.
Accepted September 4, 2002.

1535-3702/03/2281-0084$15.00

hardly be a single case. The fact that we have not found any other relevant data on the ellipticity of MVs can be explained by difficulties in determining MV sizes by such a conventional method as TEM which produces a properly magnified image and gives no bias owing to size visual estimation in optical sectioning.

Taking the above into account, an elliptical cylinder is undoubtedly preferable to a circular one in describing MV shape on limited lengths of MV basal surface. This model is indispensable when an MV is estimated to have an ellipticity of its profile obtained by sectioning perpendicular to the MV longitudinal axis (hereafter the cross-sectional profile). Besides, because this elliptical cylinder model is more general, it should be chosen in case there is no information on characteristic MV shape. The model treats MVs with circular profiles as elliptical cylinders of zero eccentricity. Nevertheless, despite all its benefits, the model practically finds no application, and the main reason for this seems to be the unknown relationships between the true (or 3-dimensional, 3D) and the section profile (or 2-dimensional, 2D) sizes in the elliptical cylinder model. As a result, it remains impossible to determine MV sizes or size distributions on the basis of the size distributions of randomly orientated MV profiles. The aim of this paper is to define these relationships and to make recommendations as to their applications.

The article consists of several parts. Part 2 presents the basic assumptions, as well as the central problem to be solved, i.e., how to define the functions that characterize the relationships between section profile sizes and the sizes of an elliptical MV (hereafter the 2D/3D functions). Part 3 deals with the central problem in connection with such size parameters as the minor radius, the major radius, the axial ratio, the area, and perimeter of a MV profile. Then, the distribution functions for the size parameters of section profiles are defined on the basis of the 2D/3D functions (Part 4). Part 4 also describes the statistical distributions of the profile sizes obtained for three-dimensionally isotropic MVs of different ellipticity. Cases of MV anisotropy are not considered in detail here, as this goes beyond the scope of our paper. Part 5 touches upon practical applications of the proposed technique, as well as gives an example of the stereological reconstruction of MVs in the rat thyroid. Finally, there follows a general discussion in Part 6.

The Model and the Problem

Basic Assumptions. (A1) The biological tissue specimen Ω under study is intersected by a plane probe Λ, and in the section $\Omega \cap \Lambda$, we can observe MV profiles. Of the sizes by which the section profiles could be described, we shall look at the minor radius Y, the major radius X, the axial ratio X/Y, the area S, and the perimeter P of the section profile. The MV sizes will be designated as Y_0, X_0, X_0/Y_0, S_0, and P_0, respectively. The sizes of the cross-sectional profiles are the same as the MV sizes; in this case, $Y = Y_0$, $X = X_0$, $X/Y = X_0/Y_0$, $S = S_0$, and $P = P_0$.

(A2) The shape of a MV on its limited lengths comparable with the X_0 value can be approximated by an elliptical, or in some particular case, by a circular cylinder. The irregularity of the outer, or basal, MV surface being negligible, it does not prevent the radii Y and X from being measured on the section.

(A3) The radius of a MV curvature on its longitudinal axis in the vicinity of a sectioning plane is greater than Y_0 by at least several times, i.e., the MV fragment being sectioned is not very curved.

To sum up, a MV is probed stereologically. The shape of a MV on its limited lengths is approximated by an elliptical cylinder with a longitudinal axis that is relatively straight in the vicinity of a sectioning plane. Numerous microanatomical data presented in the literature (e.g., Ref. 6) suggest that this shape model takes care of most MVs in different organs and tissues.

The Problem. In this study, the central problem is to identify the functions $Y = Y(X_0,Y_0,\Lambda)$, $X = X(X_0,Y_0,\Lambda)$, $X/Y = X/Y(X_0,Y_0,\Lambda)$, $S = S(S_0,\Lambda)$, and $P = P(X_0,Y_0,\Lambda)$, by means of which the sizes and/or the size distributions of elliptical MVs can be determined on the basis of size distributions of their section profiles.

Deducing the 2D/3D Functions

Let us take a single cylindrical MV whose cross-section is an ellipse, or in some particular case, a circle. The mutual orientation of the MV and the sectioning plane Λ (Fig. 1) is described by two angles α and φ, where α ($\alpha \in [0, \pi/2]$) is the angle between the MV longitudinal axis and a perpendicular to Λ, and φ ($\varphi \in [0, \pi]$) is the angle between the

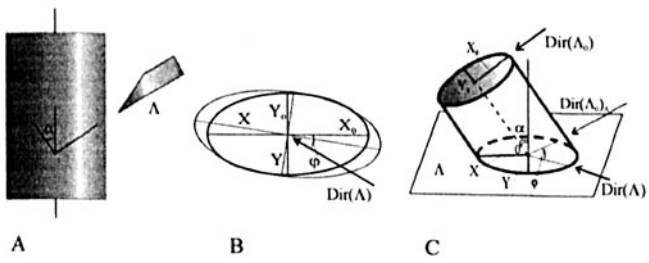

Figure 1. Angles defining the mutual orientation of a MV and a sectioning plane. (A) Side view of the MV fragment. The sectioning angle α ($\alpha \in [0, \pi/2]$) is the angle between the MV longitudinal axis and the perpendicular to the sectioning plane Λ. (B) View of the MV from above (the section profile). The ellipse with radii X_0 and Y_0 is the cross-sectional profile. Its sizes are the same as the MV sizes. If the MV is sectioned in the direction Dir(Λ), the initial profile becomes an ellipse with radii X and Y. The angle φ ($\varphi \in [0, \pi]$) is the angle between the major radius X_0 and the sectioning direction. This angle defines the direction of the profile stretching in the MV sectioning through the angle α. (C) Schematic view of the MV, the sectioning plane Λ, and the angles α and φ in 3-D space. On the cross-sectional profile (shaded), marked are the MV sizes X_0 and Y_0. Dir(Λ_0) is the direction of the major radius X_0 on the MV cross section. The sectioning of the MV in an arbitrary direction Dir(Λ) produces another elliptical profile, its major and minor radii being X and Y, respectively. Shown is the impact of the angles α and φ on the resulting differences between the sectioning directions Dir(Λ_0) and Dir(Λ). The direction $\mathrm{Dir}(\Lambda_0)_\Lambda$ is the projection of Dir(Λ_0) on the plane Λ. In calculations, MV shape was approximated by an elliptical cylinder only on limited lengths comparable with the X_0 value. For illustrative purposes, this is not so in the figures.

major radius of the cross-sectional profile and the sectioning direction Dir(Λ). So the central problem of the article, i.e., identification of the 2D/3D functions for the MV elliptical cylinder model, may be reduced to defining the expressions that describe relationships between the sizes of ellipses E and E_0, where E is the ellipse obtained from E_0 by means of the latter's stretching in an arbitrary direction Dir(Λ).

First, we define the simplest of the sought functions, i.e., the function characterizing the relationship between S and S_0. The MV sizes are the same as those of the cross-sectional profile. The latter is the orthogonal projection of a random section profile on the plane, which is perpendicular to the longitudinal axis of the MV. Thus, the sought function $S = S(S_0,\Lambda)$ does not depend on φ and can be written as:

$$S = S_0/\cos\alpha = \pi X_0 Y_0/\cos\alpha. \quad (1)$$

The functions $Y = Y(X_0,Y_0,\Lambda)$, $X = X(X_0,Y_0,\Lambda)$, $X/Y = X/Y(X_0,Y_0,\Lambda)$, and $P = P(X_0,Y_0,\Lambda)$ are defined in a more complex way because they depend not only on the sectioning angle α, but also on the sectioning direction. For instance, the equation $X = X_0/\cos\alpha$ is true only when Dir(Λ) and the direction of the major radius X_0 are the same, i.e., $\varphi = 0$. With any other φ values, X will be less than $X_0/\cos\alpha$.

To define the functions $Y = Y(X_0,Y_0,\Lambda)$, $X = X(X_0,Y_0,\Lambda)$, $X/Y = X/Y(X_0,Y_0,\Lambda)$, and $P = P(X_0,Y_0,\Lambda)$, let us take the MV cross-sectional profile as the ellipse E_0 in the coordinate system $0\vec{X}_0\vec{Y}_0\vec{Z}_0$ with the beginning in the center of the ellipse E_0 (Fig. 2A). The axis $0\vec{Z}_0$ is perpendicular to the sectioning plane Λ, the axes $0\vec{X}_0$ and $0\vec{Y}_0$ lie in Λ, and the radii X_0 and Y_0 of the ellipse are directed along the axes $0\vec{X}_0$ and $0\vec{Y}_0$, respectively. The set of the ellipse E_0 points is described by the equation:

$$\left(\frac{x_0}{X_0}\right)^2 + \left(\frac{y_0}{Y_0}\right)^2 = 1. \quad (2)$$

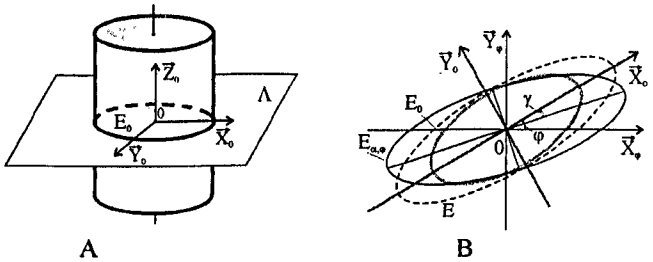

A B

Figure 2. MV section profile geometry. (A) Sectioning of the elliptical MV by the plane Λ, which is perpendicular to the longitudinal axis of the MV, produces the ellipse E_0. The coordinate system $0\vec{X}_0\vec{Y}_0\vec{Z}_0$ is shown, its beginning situated at the point of intersection of the MV longitudinal axis and the sectioning plane Λ, i.e., in the center of the ellipse E_0. The radii X_0 and Y_0 of the ellipse E_0 are directed along the axes $0\vec{X}_0$ and $\vec{Y}_0$ whereas the longitudinal axis of the MV is along $0\vec{Z}_0$. (B) The elliptical cross-sectional profile E_0 is shown in the coordinates $0\vec{X}_0\vec{Y}_0$. The coordinate system $0\vec{X}_\varphi\vec{Y}_\varphi$ is obtained by rotation of the system $0\vec{X}_0\vec{Y}_0$ through the angle φ. Stretching the ellipse E_0 by $1/\cos\alpha$ times along the axis $0\vec{X}_\varphi$ forms the ellipse $E_{\alpha,\varphi}$. The ellipse $E_{\alpha,\varphi}$ is also obtainable by rotation through the angle γ of some ellipse E with the radii X and Y directed along the axes $0\vec{X}_0$ and $0\vec{Y}_0$, respectively. Note that the direction of the major radius of the ellipse $E_{\alpha,\varphi}$ does not coincide with the direction $0\vec{X}_\varphi$, i.e., $\gamma<\varphi$.

To give the direction of ellipse E_0 stretching, which is due to the MV sectioning, let us rotate the coordinate system $0\vec{X}_0\vec{Y}_0$ through angle φ. Thus, we obtain the system $0\vec{X}_\varphi\vec{Y}_\varphi$ (Fig. 2B). The coordinates in the systems $0\vec{X}_0\vec{Y}_0$ and $0\vec{X}_\varphi\vec{Y}_\varphi$ are connected by the formulae:

$$\begin{cases} x_0 = x_\varphi\cos\varphi - y_\varphi\sin\varphi \\ y_0 = x_\varphi\sin\varphi + y_\varphi\cos\varphi. \end{cases} \quad (3)$$

After the substitution into Equation 2, we have for the ellipse E_0 in the coordinates $0\vec{X}_\varphi\vec{Y}_\varphi$

$$\frac{1}{X_0^2}\cdot(x_\varphi\cos\varphi - y_\varphi\sin\varphi)^2 + \frac{1}{Y_0^2}\cdot(x_\varphi\sin\varphi + y_\varphi\cos\varphi)^2 = 1, \quad (4)$$

$$\left(\frac{\cos^2\varphi}{X_0^2} + \frac{\sin^2\varphi}{Y_0^2}\right)\cdot x_\varphi^2 - 2\cdot\left(\frac{1}{X_0^2} - \frac{1}{Y_0^2}\right)\sin\varphi\cdot\cos\varphi\cdot x_\varphi \cdot y_\varphi + \left(\frac{\sin^2\varphi}{X_0^2} + \frac{\cos^2\varphi}{Y_0^2}\right)\cdot y_\varphi^2 = 1. \quad (5)$$

Let a quantity Δ_0 be:

$$\Delta_0 = \frac{1}{Y_0^2} - \frac{1}{X_0^2}, \text{ i.e., } \frac{1}{X_0^2} = \frac{1}{Y_0^2} - \Delta_0. \quad (6)$$

After its substitution into (5), we can write down:

$$\left(\frac{1}{Y_0^2} - \Delta_0\cdot\cos^2\varphi\right)\cdot x_\varphi^2 + 2\Delta_0\cdot\sin\varphi\cdot\cos\varphi\cdot x_\varphi\cdot y_\varphi + \left(\frac{1}{Y_0^2} - \Delta_0\cdot\sin^2\varphi\right)\cdot y_\varphi^2 = 1. \quad (7)$$

By stretching the ellipse E_0 presented in the coordinates $0\vec{X}_\varphi\vec{Y}_\varphi$ by $1/\cos\alpha$ times along the axis $0\vec{X}_\varphi$ (Fig. 2B), we get the ellipse $E_{\alpha,\varphi}$ whose points satisfy the following equation:

$$\cos^2\alpha\cdot\left(\frac{1}{Y_0^2} - \Delta_0\cdot\cos^2\varphi\right)\cdot x_\varphi^2 + 2\Delta_0\cos\alpha\cdot\sin\varphi\cdot\cos\varphi\cdot x_\varphi\cdot y_\varphi + \left(\frac{1}{Y_0^2} - \Delta_0\cdot\sin^2\varphi\right)\cdot y_\varphi^2 = 1. \quad (8)$$

We might obtain the same ellipse $E_{\alpha,\varphi}$ by rotation through the angle γ of some ellipse E whose radii X and Y are directed along the axes $0\vec{X}_0$ and $0\vec{Y}_0$, respectively. It follows from Equation 7 that for the ellipse E:

$$\left(\frac{1}{Y^2} - \Delta\cdot\cos^2\gamma\right)\cdot x^2 + 2\Delta\cdot\sin\gamma\cdot\cos\gamma\cdot x\cdot y + \left(\frac{1}{Y^2} - \Delta\cdot\sin^2\gamma\right)\cdot y^2 = 1, \text{ where } \Delta = \frac{1}{Y^2} - \frac{1}{X^2}. \quad (9)$$

Comparing the equations for the ellipses $E_{\alpha,\varphi}$ (8) and E (9), we obtain the system:

$$\begin{cases} \frac{1}{Y^2} - \Delta\cdot\cos^2\gamma = \cos^2\alpha\cdot\left(\frac{1}{Y_0^2} - \Delta_0\cdot\cos^2\varphi\right) \\ \Delta\cdot\sin\gamma\cdot\cos\gamma = \cos\alpha\cdot\Delta_0\cdot\sin\varphi\cdot\cos\varphi \\ \frac{1}{Y^2} - \Delta\cdot\sin^2\gamma = \frac{1}{Y_0^2} - \Delta_0\cdot\sin^2\varphi. \end{cases} \quad (10)$$

Its solution is the expression relating the size Y_0 of the initial ellipse E_0 (or the minor radius of the cross-sectional profile) to the size Y of the ellipse $E_{\alpha,\varphi}$ obtained from the ellipse E_0 by its stretching by $1/\cos\alpha$ times in the arbitrary direction Dir(Λ) (or the minor radius of the random MV profile), i.e., the sought function $Y = Y(X_0,Y_0,\Lambda)$:

$$Y = \left[\frac{X_0^2(1 + 1/\cos^2\alpha) - (X_0^2 - Y_0^2)\cdot(\cos^2\varphi + \sin^2\varphi/\cos^2\alpha)}{2} - \sqrt{\frac{[X_0^2(1 + 1/\cos^2\alpha) - (X_0^2 - Y_0^2)\cdot(\cos^2\varphi + \sin^2\varphi/\cos^2\alpha)]^2}{4} - \frac{X_0^2Y_0^2}{\cos^2\alpha}}\right]^{0.5}. \quad (11)$$

The function is in its analytic form, which means that any of its values is calculable in case X_0, Y_0, and Λ are known. X_0, Y_0, and Λ may be defined either as constants or by random quantities with given distributions. Specifically, the mutual orientation of the MV and the sectioning plane Λ may be described by the distribution function $\Lambda = G_\Lambda(\alpha,\varphi)$.

Similarly, we can define the function describing the relationship between the profile major radius X and the true major radius X_0. It will be more convenient, however, to use the ellipse area formula (1). Hence, X makes up:

$$X = \frac{X_0Y_0}{\cos\alpha\cdot Y(X_0, Y_0, \Lambda)}. \quad (12)$$

Further, we define the sought function for the axial ratio:

$$\frac{X}{Y} = \frac{X_0Y_0}{\cos\alpha\cdot[Y(X_0, Y_0, \Lambda)]^2} \quad (13)$$

and for the perimeter of the section profile:

$$P = Y\cdot\int_0^{2\pi}\sqrt{\cos^2\zeta + \left(\frac{X}{Y}\sin\zeta\right)^2}\,d\zeta = Y(X_0, Y_0, \Lambda)\cdot \int_0^{2\pi}\sqrt{\cos^2\zeta + \frac{X_0^2\cdot Y_0^2\cdot\sin^2\zeta}{\cos^2\alpha\cdot[Y(X_0, Y_0, \Lambda)]^4}}d\zeta, \quad (14)$$

where ζ is the angle characterizing the position of a point on the ellipse contour against the major radius X.

Statistical Distributions of the Sizes of MV Section Profiles

As has been noted above, the mutual orientation of a MV and a sectioning plane is described by the angles α and φ, with α defining the degree of MV profile stretching, and φ defining the direction of stretching. The known values of Y_0, X_0, the stretching degree $1/\cos\alpha$, and the direction of stretching φ make it possible to estimate any of the studied size parameters. Specifically, the orientation of a MV against a sectioning plane being described by the distribution function $G_\Lambda(\alpha,\varphi)$, the following cumulative distribution function [CDF(b), or CDF] for the minor radius of MV section profiles is determined by:

$$CDF_Y(b) = \int_0^{\pi/2}\int_0^{2\pi} h[Y(X_0,Y_0,\Lambda), b]dG_\Lambda(\alpha,\varphi), \quad (15)$$

where $h[Y(X_0,Y_0,\Lambda), b]$ is the Heaviside step function, which is equal to 1 provided $Y(X_0,Y_0,\Lambda)\le b$ or is equal to 0 otherwise.

Similarly, we can get the CDFs for the major radius:

$$CDF_X(b) = \int_0^{\pi/2}\int_0^{2\pi} h\left[\frac{X_0Y_0}{\cos\alpha\cdot Y(X_0,Y_0,\Lambda)}, b\right]dG_\Lambda(\alpha,\varphi), \quad (16)$$

for the axial ratio:

$$CDF_{X/Y}(b) = \int_0^{\pi/2}\int_0^{2\pi} h\left[\frac{X_0Y_0}{[Y(X_0,Y_0\Lambda)]^2\cdot\cos\alpha}, b\right]dG_\Lambda(\alpha,\varphi), \quad (17)$$

for the area:

$$CDF_S(b) = \int_0^{\arccos(S_0/b)}\int_0^{2\pi}\frac{S_0}{\cos\alpha}, dG_\Lambda(\alpha,\varphi) \quad (18)$$

and for the perimeter of a MV profile:

$$CDF_P(b) = \int_0^{\pi/2}\int_0^{2\pi} h\left[Y(X_0,Y_0,\Lambda)\cdot \int_0^{2\pi}\sqrt{\cos^2\zeta + \frac{X_0^2\cdot Y_0^2\cdot\sin^2\zeta}{\cos^2\alpha\cdot[Y(X_0,Y_0,\Lambda)]^4}}\,d\zeta, b\right]dG_\Lambda(\alpha,\varphi). \quad (19)$$

The probability density functions (PDFs) for the studied size parameters can be expressed as derivatives of the corresponding CDFs:

$$PDF_Y = \frac{dCDF_Y}{db}, PDF_X = \frac{dCDF_X}{db}, PDF_{X/Y} = \frac{dCDF_{X/Y}}{db}, PDF_S = \frac{dCDF_S}{db}, PDF_P = \frac{dCDF_P}{db}. \quad (20)$$

Moments (M_n) and central moments (μ_n) of the statistical distributions are defined in the standard way, e.g., for the minor radius of a MV profile we have:

$$M_n(Y) = \int_0^{\pi/2}\int_0^{2\pi}[Y(X_0,Y_0,\Lambda)]^n dG_\Lambda(\alpha,\varphi), \text{ and } \mu_n(Y) = \int_0^{\pi/2}\int_0^{2\pi}[Y(X_0,Y_0,\Lambda) - M(Y)]^n dG_\Lambda(\alpha,\varphi). \quad (21)$$

Let us present graphically the distributions of the studied size parameters of MV profiles. We shall examine cases of different fixed ellipticity of the MVs given $Y_0 = 1.0$ and X_0 is equal to 1.0, 1.5, 2.0, 3.0, 5.0, or 7.0. To plot the

graphs, the function for the angles α and φ joint distribution has to be defined as well. This function $G_\Lambda(\alpha,\varphi)$ could describe the degree of anisotropy that is intrinsic to the mutual orientation of a MV and a sectioning plane. The deduced formulae imply the possibility of introducing any distribution function as $G_\Lambda(\alpha,\varphi)$ provided $\alpha\in[0, \pi/2]$ and $\varphi\in[0, \pi]$, e.g., Dimroth-Watson function of the axial distribution was used by Cruz-Orive *et al.* (7) in the investigation of the length and surface densities of skeletal muscle capillaries. However, for illustrative purposes, we shall take the simplest case, the one with zero anisotropy implying the random independent orientation of MVs in tissue volume along with the random independent orientation of sectioning planes. Under these conditions, the angle α is characterized by 3D isotropy, and its PDF_α is equal to $\sin\alpha$ ($PDF_\alpha = \sin\alpha$, $\alpha\in[0, \pi/2]$; consequently, $CDF_\alpha = 1-\cos\alpha$). The angle φ possesses 2D isotropy, which means that the distribution of the angle φ is uniform ($PDF_\varphi = \text{const}$, $\varphi\in[0, \pi]$; hence, $CDF_\varphi \sim \varphi$). This case can be used, in the first place, to analyze the characteristic shape of the curves of the distribution functions studied. It can also be of considerable practical importance because abundant microanatomical data make it possible to regard, on the first approximation, the MVs of the endocrine glands, prostate, liver, spleen, lung, mammary gland, pancreas, brain, autonomic ganglia, thymus, lymphatic nodes, spongy bones, and some other organs as three-dimensionally isotropic (e.g., Ref. 6).

Under the defined conditions, the PDF curves have been plotted for the studied size parameters of MV section profiles (Fig. 3). The size class width was equal to 0.01. The calculation error was not more than 0.0075 of the characteristic value for X/Y and 0.0025 for the other size parameters under study. Each of the obtained curves demonstrates an infinite maximum whose abscissa is equal to the true value of the size. On the graphs of the PDF_Y (Fig. 3A), local maximums have been found in the vicinity of $Y = X_0$, but they are expressed only slightly, being almost indistinguishable from the abscissa axis provided $X_0 \geq 3.0$. The local maximums are due to the fact that the major radius X_0 is seen as the minor radius Y on the profiles considerably stretched in the direction close to the minor radius Y_0. In addition to PDFs, Figure 3D demonstrates the $CDF_{X/Y}$ curves. It should be noted that the vertical parts of these curves correspond to the true values of the MV axial ratio.

The fact that the Y, X, X/Y, S, and P distribution modal values are equal to the respective true values Y_0, X_0, X_0/Y_0,

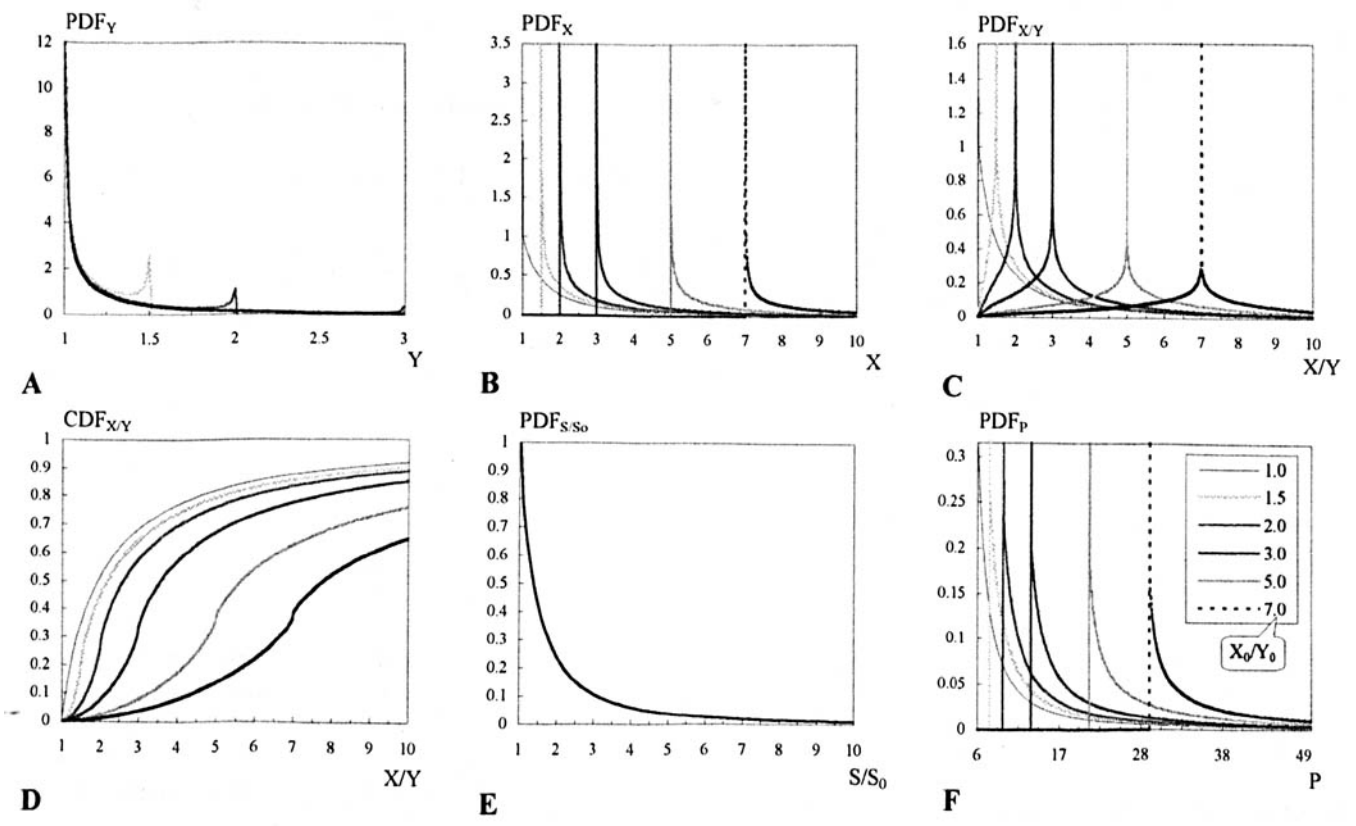

Figure 3. Size distributions of the MV section profiles. Shown are the plots of PDFs for the minor (A) and major (B) radii of the MV profiles, the $PDF_{X/Y}$ (C), the $CDF_{X/Y}$ (D), the PDFs of S/S_0 (E), and of the perimeter (F) at different X_0/Y_0 values. The shape of the curve on the graph E does not depend on X_0/Y_0. The interval $(-\infty, 1)$ is not included in the argument area of the functions $Y = Y(X_0,Y_0,\Lambda)$, $X = X(X_0,Y_0,\Lambda)$, $X/Y = X/Y(X_0,Y_0,\Lambda)$, and $P = P(X_0,Y_0,\Lambda)$ because the profiles with $Y < 1.0$, $X < 1.0$, $X/Y < 1.0$, or $P < 1.0$ do not occur when $Y_0=1.0$ and $X_0\geq 1.0$. S/S_0 cannot be less than 1 either. The PDF curves have an infinite maximum whose abscissa is equal to the true value of the size measured. The $CDF_{X/Y}$ curves display the vertical parts corresponding to the $PDF_{X/Y}$ maximums. Some parts of the PDF curves, especially on A, lie so close to each other that they are almost indistinguishable. The PDF_Y curve for $X_0/Y_0=1.0$ is nonexistent because $Y = 1$ in this case. With the scale used in this graph, the PDF_Y is close to zero when $Y \geq 3.0$ (not shown).

S_0, and P_0 should be stressed because of its practical importance. The mechanism of this phenomenon can briefly be explained as follows. In spherical coordinates, with $\alpha \rightarrow 0$, the sphere region corresponding to the interval of the angle φ values tends to a point. An infinite amount of φ values in the interval from 0 to π produces an infinite PDF. It follows from this that plotting PDF curves for other size parameters (e.g., a curvature of the profile contour) will give the modal values equal to the true values of the sizes. This is so if the PDF curve shapes are not changed greatly by the function $G_\Lambda(\alpha,\varphi)$, i.e., MVs do not possess severe anisotropy.

Some Practical Aspects and an Example

The obtained 2D/3D functions make it possible to calculate the size distributions of section profiles for MVs of any known sizes. The PDFs of Y, X, X/Y, S, and P can be determined, along with distribution function parameters including the mode, mathematical expectation, variance, and other moments of the distributions, with Y_0, X_0, X_0/Y_0, S_0, P_0, α, and φ being given as either constants or quantity intervals described by some statistical distributions. For instance, the PDF curves shown in Figure 3 have been plotted for the three-dimensionally isotropic MVs of the fixed sizes. The other model curves are obtainable in the same way. Their comparison with the factual distributions of Y, X, X/Y, S, and P contributes to solving the practical task of estimating the characteristic value of the sizes and the special features of MV size distribution, which is the subject of this paper.

Of great importance is the fact that PDF curves can also be plotted for more complex cases in which the distributions of Y_0, X_0, X_0/Y_0, S_0, P_0, α, and φ could be different from the ones given above. This might prove to be necessary if any significant discrepancy should be discovered by the researcher between the factual data and the model curves plotted. It must be noted in this respect that when the size parameter acquires some variance, the PDF maximum will be smeared. The degree of this smearing will depend on the variance value. Multiple maximums will appear in case of discrete variants, or clusters, of MVs in the tissue. The abscissa of each of the maximums will be equal to the characteristic size value inside the cluster. As in unimodal distribution, should there appear a size parameter variance, each of the multiple maximums of the PDF curve will demonstrate the smearing.

We have applied the proposed technique of determining MV sizes in the study of thyroid perifollicular hemocapillaries. Our purpose was to estimate the characteristic value (or values) of the MV axial ratio X_0/Y_0. Four male albino rats were selected for this study (body weight, 243 ± 11.3 g, ± SEM). With the animals under ether anesthesia, the specimens of the thyroids were excised and consecutively fixed in glutaraldehyde (2.5% for 2 hr) and osmium tetroxide (1% for 1 hr) in cacodylate buffer (pH 7.4). Obtained on the LKB microtome, the ultrathin sections were contrasted for TEM by uranyl acetate and lead citrate. The H-300 microscope (Hitachi, Tokyo, Japan) was used for section observation and morphometry. On microphotographs with the final magnification of ×1650, the minor Y and the major X radii were measured on 100 randomly chosen capillary profiles (25 profiles from each rat). All measurements were made manually by the same researcher.

Most of the MV profiles obtained were of a regular enough elliptical shape. If they were to be approximated by an ellipse of the same area, the X and Y values would deviate from the measured ones by no more than 10%. Other features of the profiles also suggested that in immersion fixation the capillaries were not collapsed appreciably. Specifically, red blood cells were rarely found in the capillary lumen. Whenever they were actually present in the lumen, they never filled the latter completely.

On the basis of the measurements, a histogram for the frequency of X/Y classes was constructed (Fig. 4). The histogram had a maximum whose abscissa was equal to 1.6. Then, a theoretical histogram of X/Y was constructed for the three-dimensionally isotropic capillaries with the axial ratio of $X_0/Y_0 = 1.6$ and zero variance of this size [$\mathrm{Var}(X_0/Y_0) = 0$]. The agreement of the factual data with the model has been revealed visually. However, the factual frequency of the profiles with $1.0 \leq X/Y < 1.2$ was higher than expected, and the χ^2_{28} value was high ($\chi^2_{28} = 45.425$, $P = 0.020$ – the probability that the null hypothesis is true). This suggested the presence of a cluster of circular MVs in the thyroids. Indeed, the introduction in the model of a cluster with circular capillaries (its size being equal to 19.5% of the total number of the capillaries) increased the accuracy of the fitting ($\chi^2_{28} = 22.428$, $P = 0.761$). A still better fit to the factual data was found when an additional cluster was introduced with $X_0/Y_0 = 3.2$ to explain the outbreak at $3.2 \leq X/Y < 3.4$. We obtained $\chi^2_{28} = 18.124$, $P = 0.923$, when 72.7% of the thyroid capillaries had the $X_0/Y_0 = 1.6$ flatness, 17.6% were circular in their cross-sectional profiles ($X_0/Y_0 = 1.0$), and 9.7% had the axial ratio of $X_0/Y_0 = 3.2$. The variance of the capillaries on X_0/Y_0 inside the clusters, as well as their anisotropy, was negligibly small. In other words, the capillaries inside the clusters of the model have the same X_0/Y_0 values.

It is noteworthy that the quality of fitting of the thyroid capillaries could be increased even with the current number of section profiles. For example, this could be achieved by introducing a certain variance inside a cluster with $X_0/Y_0 = 1.6$, which could explain it why factual frequencies are somewhat higher than expected for size classes $1.4 \leq X/Y < 1.6$ and $1.8 \leq X/Y < 2.0$. In our case, however, the study of thyroid capillaries is mainly of illustrative importance. A special study based on more factual data will be the purpose of the next paper.

Furthermore, it should be noted that the reconstruction of the MV sizes from the size distributions of section profiles is also possible without constructing frequency histograms, the moments and the central moments of the distributions being used for this purpose. The accuracy of size

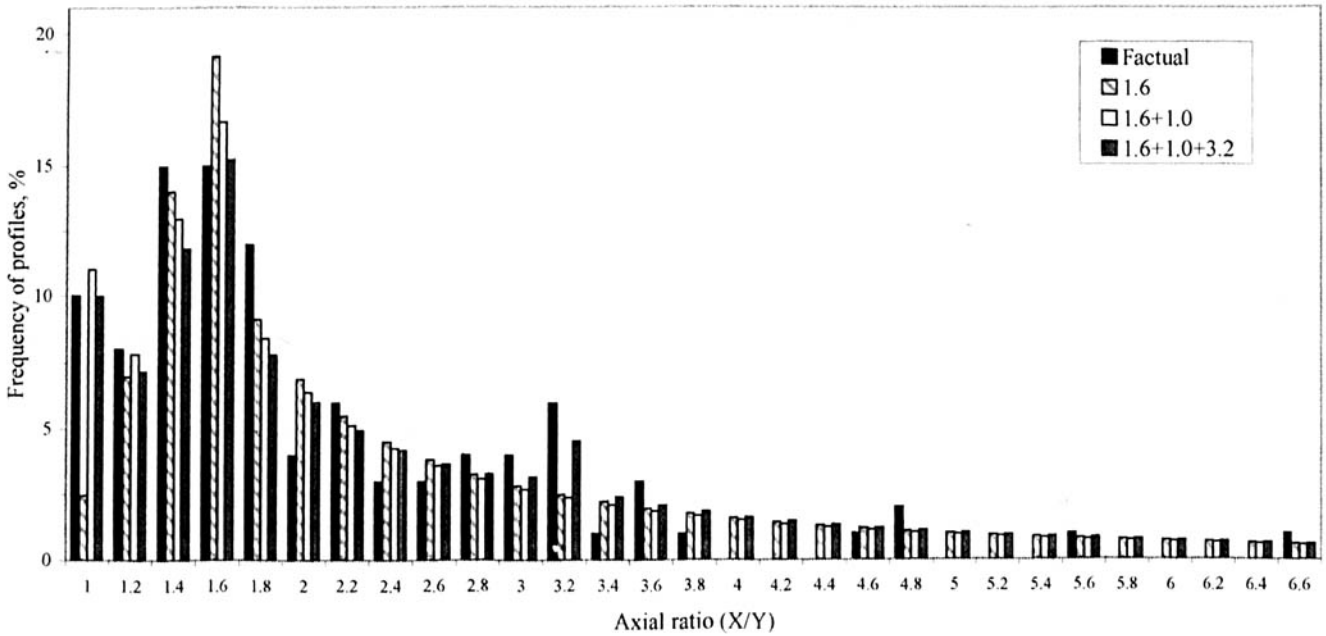

Figure 4. Distribution of axial ratios of perifollicular capillary profiles in the rat thyroid. The factual distribution (black bars) shows the highest frequency of the profiles with axial ratios $1.4 \leq X/Y < 1.6$ and $1.6 \leq X/Y < 1.8$. Therefore, the mode of the factual distribution is located in the vicinity of 1.6. A theoretical histogram was constructed for the three-dimensionally isotropic capillaries with $X_0/Y_0 = 1.6$ and $Var(X_0/Y_0) = 0$ (series "1.6"). Its maximum does not achieve infinity because the histogram class width (=0.2) is larger than zero. After introducing a cluster of circular MVs (the cluster size equals 19.5% of the total number of the capillaries; series "1.6 + 1.0"), the factual and the theoretical histograms are in rather good agreement at $P = 0.761$. A still better fit ($P = 0.923$) is found when 17.6% of the capillaries have no ellipticity of the cross-sectional profile ($X_0/Y_0 = 1.0$); 72.7% have a flatness $X_0/Y_0 = 1.6$, and 9.7%, $X_0/Y_0 = 3.2$ (series "1.6 + 1.0 + 3.2").

estimates obtained by the method of moments is smaller because the moments of the second and higher orders are usually estimated with large standard errors and with a severe bias due to the missing profiles (e.g., Ref. 8). Besides, the values of the moments may depend in a way on the function $G_\Lambda(\alpha,\varphi)$. Therefore, the method of moments should be used only if rough estimates of the MV sizes are to be obtained.

Discussion

Cylindrical objects are not infrequently found in living organisms, as well as in natural and technical systems. So, quite understandably, investigators pay considerable attention to their stereology. There are many publications on the subject. Some are devoted to relationships between the sizes of cylindrical objects and the sizes of their projections on a plane (e.g., Refs. 9–12), which is typical of materials sciences. Other papers examine relationships between the sizes of cylindrical objects and the sizes of their section profiles (e.g., Refs. 4 and 13–19). This approach is mainly applied to biological and medical objects.

Most of the above-mentioned publications focus on the stereology of circular cylindrical objects. Among the papers that have come to our notice, only the ones by Hennig and Elias (20) and Elias and Hyde (16) touch upon the stereology of elliptical cylinders. The authors have looked at the relationships between the 3D and 2D values, the latter were defined on section profiles, for the axial ratio, which is one of the size parameters we have studied. In Reference 20, the $CDF_{X/Y}$ curves have been obtained for elliptical cylinders of some fixed axial ratios. In Reference 16, the X/Y histograms for the true axial ratios equal to 1.0, 2.0, and 4.0 have been constructed. These histograms have been suggested for rough estimation of the ellipticity of a cylindrical object under study by comparing them with the factual data. In general, the findings in the articles referred to are in quite good agreement with ours. But in Reference 20, the $CDF_{X/Y}$ curves do not have the vertical parts and, therefore, the maximal PDFs will not be infinite (compare Fig. 3, C and D). This discrepancy may be accounted for by the degree of statistical modeling accuracy achievable several decades ago, as well as by a rather large size class width used by the researchers.

In this paper, we present the technique for determining elliptical MV size distributions on the basis of MV profile size distributions. The defined 2D/3D functions underlie a novel approach to stereological reconstruction in microangiology, making it possible to develop more precise models of MVs and microcirculatory networks. The technique can be applied to networks with any given kind of MV size distributions. The obtained 2D/3D functions are universal and can readily be used in different disciplines concerned with estimating object sizes on their section profiles, in case an object shape on its limited lengths is approximated with the required accuracy by an elliptical cylinder. Thus, the technique has a wide range of applications. The fact that it is proposed to be used in MV studies is explained exclusively by our research objectives.

The technique is classified as one of the model-based methods that are, as is known, of diminished use in modern research. However, its application in this case is justified because none of the existing design-based methods can give an idea of the size, let alone size distributions, of MV cross-sectional profiles. This information is necessary to develop structural and functional models of microcirculatory networks. Therefore, we have every reason to believe that this technique will be widely used in microangiology.

The proposed technique is based on several assumptions about a MV shape. The first of them implies that MVs on their limited lengths are studied as elliptical cylinders with a relatively smooth basal surface. At the same time, the irregularity of the MV contour, if any, only slightly restricts the applicability of the technique. The PDF curves of the size parameters under study, and especially infinite maximums of the curves, are robust enough to a MV shape deflection. The influence of this deflection decreases still further due to the chosen procedure of the size distribution fitting, which can reduce certain noises.

Furthermore, we have assumed in A3 that the sectioned fragment of a MV should not be very curved. The radius of a MV curvature on its longitudinal axis in the vicinity of a sectioning plane should be greater than Y_0 by at least several times. Otherwise, there will appear profiles of irregular shape on which the radii can be measured only with a severe bias. As a result, the factual distributions of the size parameters will differ from the expected ones. For this reason, the proposed technique should not be employed in studies of glomerular capillaries and other MVs that regularly have an expressed curvature. Still, the assumed absence of a marked curvature does not make it necessary to view MVs as a set of long straight cylinders. In most cases, such a description of MVs would be erroneous and result only in unsatisfactory fitting of MV size distribution. Instead, we regard MVs as a set of short, and relatively straight elliptical cylinders, sectioned by planes at any point other than their ends. Certainly, long, straight cylinders can also be described by the above set. More importantly, though, is the fact that the set makes it possible to describe complex networks of MVs that possess, specifically, a curvature along the longitudinal axis. However, the curvature should not be too pronounced, and there should be no other factors that could lead to a significant deviation of section profile shape from an ellipse. Our belief is that such a description of MVs meets the needs of modern microangiology.

One more assumption made in this paper concerns section thickness. Because in A1, a plane probe has been used to generate sections, the MV profiles are regarded as 2D objects. It should be noted that the assumption of section zero thickness is not unusual for stereology (e.g., Refs. 21–24). This is done to avoid biases emerging in calculations when a section thickness and an object size should become comparable in value. The considered case of the TEM of MVs does not contradict A1 because the thickness of an ultrathin section (40 ÷ 80 nm) is much smaller than any MV minor radius Y_0 ($\geq$2.0 μm). In this connection, the proposed technique seems to be a powerful tool in MV modeling in view of the expected development of ultra-high-resolution scanners in computed tomography, magnetic resonance imaging, and confocal laser scanning microscopy. These apparatuses will produce MV profile images corresponding to sections of very small or even zero thickness.

In our calculations, we have used the single cylinder approach, which is known to be the standard procedure in stochastic geometry and geometrical probability. To bend the shape model toward a reality in which a number of MVs are studied, it is necessary to identify the distribution function of the size parameter under investigation and the distribution function of the angles $G_\Lambda(\alpha,\varphi)$ that defines the mutual orientation of a MV and a sectioning plane. For example, the curves in Figure 3 have been plotted for the profile size parameters, the sectioning of a single MV (or of MVs of the same size) being random independent. This model is ideal, but it serves as a starting point in factual data interpreting. If need be, the required distributions of MV sizes can be implicated, as well as the angular distribution $G_\Lambda(\alpha,\varphi)$ to define an anisotropy of studied MVs. This is essential when the confidence probability $P(\chi^2)$ is unacceptably low.

The technique of stereological reconstruction we propose implies obtaining model distribution of the size or sizes of MV section profiles that steadily approaches factual distribution due to the introduction of complicating factors. In our example, we started with constructing the X/Y theoretical histogram for the three-dimensionally isotropic thyroid capillaries with the same axial ratio of $X_0/Y_0 = 1.6$. We then added a cluster of capillaries with $X_0/Y_0 = 1.0$. Finally, the model X/Y distribution was refined by employing a small cluster of capillaries with $X_0/Y_0 = 3.2$. The resultant model, which can be considered as a statistical estimate of MVs under study, included three clusters of the capillaries, their X_0/Y_0 values inside the clusters being fixed. By introducing the size clusters, we have complicated the model, thereby increasing the confidence probability $P(\chi^2)$, and therefore making it possible to better fit the X/Y factual histogram.

In other words, the procedure of MV factual size distribution fitting is iterative. Like in other iterations, in the presence of all the substantial factors, the $P(\chi^2)$ increment is insignificant. In this case, the unexplained deviations of section profile frequencies from the expected ones are merely the stochastic model noise resulting from different unaccounted-for factors. Among these are inaccuracies in section profile measurements that may be due to the inadequate resolution of digitized profile images; deviation of MV shape from the assumed one; and complexity of factual size and/or angular distributions. Although noise analysis in this novel type of MV structural models merits a separate paper, it should be borne in mind that if the overall noise in the resultant model is low, i.e., if $P(\chi^2)$ is high, the impact

of each disturbing factor can also, on the whole, be thought of as low. The concept of noise analysis in stochastic models used to evaluate the impact of disturbing factors has been examined in considerable detail in our previous articles devoted to the study of C-cell-blood calcitonin transport in the rat thyroid (25, 26). In the present study of the capillaries, the $P(\chi^2)$ value achieved was equal to 0.923. This confidence probability is high enough for purposes of approximation rather than for estimating statistical differences, which suggests that the conditions used in modeling are quite adequate. Specifically, this is true of the shape of blood capillaries in the rat thyroid, as well as of their size clustering and three-dimensionally isotropic arrangement.

In conclusion, it should be noted that of particular interest is the shape of the $PDF_{X/Y}$ curves for MVs with $1.0 < X_0/Y_0 \leq 3.0$. In this biologically most relevant case of MV ellipticity, the frequency histograms of X/Y seem to be very similar to lognormal distributions often referred to in scientific literature (e.g., Refs. 27 and 28). However, the X/Y distributions are not lognormal. Their maximal PDFs are equal to infinity, whereas lognormal distribution has a finite maximal PDF value. There are also some differences in the curvature of the $PDF_{X/Y}$ and $CDF_{X/Y}$ lines, as well as in their asymptotics. If disregarded, these differences could result in significant errors in MV modeling.

1. Howard CV, Reed MG. Unbiased Stereology. Three-Dimensional Measurement in Microscopy. RMS Handbook 41. Oxford, UK: BIOS Scientific Publishers, 1998.
2. Bishop SP, Powell PC, Hasebe N, Shen YT, Patrick TA, Hittinger L, Vatner SF. Coronary vascular morphology in pressure-overload left ventricular hypertrophy. J Mol Cell Cardiol **28:**141–154, 1996.
3. Damiano ER. The effect of the endothelial-cell glycocalyx on the motion of red blood cells through capillaries. Microvasc Res **55:**77–91, 1998.
4. Krasnoperov RA, Grachev SV, Gerasimov AN. [Errors in measurement of section areas and perimeters of MVs from their profiles in sections for light and electron microscopy]. Biofiz **46:**530–536, 2001.
5. Kassab GS, Lin DH, Fung Y-CB. Morphometry of pig coronary venous system. Am J Physiol **267:**H2100–H2113, 1994.
6. Ross MH, Romrell LJ, Kaye GI. Histology: A Text and Atlas (3rd ed). Baltimore, MD: Williams & Wilkins, 1995.
7. Cruz-Orive LM, Hoppeler HM, Mathieu O, Weibel ER. Stereological analysis of anisotropic structures using directional statistics. Appl Statist **34:**14–32, 1985.
8. Cruz-Orive LM. Distribution-free estimation of sphere size distributions from slabs showing over-projection and truncation, with a review of previous methods. J Microsc **131:**265–290, 1983.
9. Beunder EM, Rem PC. Screening kinetics of cylindrical particles. Int J Miner Process **57:**73–81, 1999.
10. Serganov VF, Likhtenshtein GI, Levchenko LA. [Determination of the electrondensity particles from electron microphotographs. The method of function of areas distribution]. Biofiz **40:**361–364, 1995.
11. Vickers GT. The projected areas of ellipsoids and cylinders. Powder Technol **86:**195–200, 1996.
12. Vickers GT, Brown DJ. The distribution of projected area and perimeter of convex, solid particles. Proc R Soc Lond **A457:**283–306, 2001.
13. Adair TH, Wells ML, Hang J, Montani JP. A stereological method for estimating length density of the arterial vascular system. Am J Physiol **266:**H1434–H1438, 1994.
14. Baddeley A, Awerback P. Stereology of tubular structures. J Microsc **131:**323–340, 1983.
15. Elias H. Stereology of parallel, straight, circular cylinders. J Microsc **107:**199–202, 1976.
16. Elias H, Hyde DM. An elementary introduction to stereology (quantitative microscopy). Am J Anat **159:**412–446, 1980.
17. Jurgen H. Estimation of tubule or cylinder L_V, S_V and V_V on thick sections. J Microsc **117:**333–345, 1979.
18. Mattfeldt T. Estimation of length and surface of anisotropic capillaries. J Microsc **135:**181–190, 1984.
19. Mayhew TM. Geometric model of the rat intestinal mucosa for stereological evaluation of villus amplification factors. J Microsc **135:**337–346, 1984.
20. Hennig A, Elias H. Elliptical cylinders. Z Wiss Mikrosk **66:**226–234, 1964.
21. Cruz-Orive LM. Particle size-shape distributions: the general spheroid problem. I. Mathematical model. J Microsc **107:**235–253, 1976.
22. Kanatani K-I. Procedures for stereological estimation of structural anisotropy. Int J Eng Sci **23:**587–598, 1985.
23. Przystupa MA. Estimation of true size distribution of partially aligned same-shape ellipsoidal particles. Scripta Mater **37:**1701–1707, 1997.
24. Sahagian DL, Proussevitch AA. 3D particle size distributions from 2D observations: stereology for natural applications. J Volcanol Geotherm Res **84:**173–196, 1998.
25. Krasnoperov RA. Biological availability of endogenous calcitonin in rats. Bull Exp Biol Med **130:**1024–1026, 1998.
26. Krasnoperov RA, Grachev SV, Glumova VA, Gerasimov AN, Ryashchikov SN. Efficiency of the calcitonin-transporting activity of the hemato-C-cellular system in the thyroid gland. Biol Bull **4:**382–386, 1997.
27. Aligizaki KK, Cady PD. Air content and size distribution of air voids in hardened cement pastes using the section-analysis method. Cem Concr Res **29:**273–280, 1999.
28. Kuhnle GE, Groh J, Leipfinger FH, Kuebler WM, Goetz AE. Quantitative analysis of network architecture, and microhemodynamics in arteriolar vessel trees of the ventilated rabbit lung. Int J Microcirc Clin Exp **12:**313–324, 1993.